Flume Testing of Passively Adaptive Composite Tidal Turbine Blades under Combined Wave and Current Loading

Kate E. Porter[a], Stephanie E. Ordonez-Sanchez[a]*, Robynne E. Murray[b], Matthew Allmark[c], Cameron M. Johnstone[a], Tim O'Doherty[c], Allan Mason-Jones[c], Darrel A. Doman[b], Michael J. Pegg[b]

[a]Energy Systems Research Unit, University of Strathclyde, Glasgow G1 1XJ, Scotland, UK

[b]Department of Mechanical Engineering, Dalhousie University, PO Box 15000, Halifax, Nova Scotia B3H 4R2, Canada

[c]School of Engineering, Cardiff University, Queen's Buildings, The Parade, Cardiff CF24 3AA, Wales, UK

*Corresponding author: s.ordonez@strath.ac.uk

Abstract— The tidal energy industry is progressing rapidly, but there are still barriers to overcome to realise the commercial potential of this sector. Large magnitude and highly variable loads caused by waves acting on the turbine are of particular concern. Composite blades with in-built bend-twist elastic response may reduce these peak loads, by passively feathering with increasing thrust. This could decrease capital costs by lowering the design loads, and improve robustness through the mitigation of pitch mechanisms. In this study, the previous research is extended to examine the performance of bend-twist blades in combined wave-current flow, which will frequently be encountered in the field. A scaled 3 bladed turbine was tested in the flume at IFREMER with bend-twist composite blades and equivalent rigid blades, sequentially under current and co-directional wave-current cases. In agreement with previous research, when the turbine was operating in current alone at higher tip speed ratios the bend-twist blades reduced the mean thrust and power compared to the rigid blades. Under the specific wave-current condition tested the average loads were similar on both blade sets. Nevertheless, the bend-twist blades substantially reduced the magnitudes of the average thrust and torque fluctuations per wave cycle, by up to 10% and 14% respectively.

Keywords—Composite blades; dynamic loading; laboratory flume; passively adaptive blades; tidal turbine; wave-current interactions

NOMENCLATURE

BT	Bend-twist
CM	Current tests with wave maker installed
CO	Current tests (undisturbed)
CMM	Coordinate measuring machine
C_P	Power coefficient
C_T	Thrust coefficient
FFT	Fast Fourier transform
HATT	Horizontal axis tidal turbine
LDV	Laser Doppler velocimeter
PSD	Power spectral density
Re	Reynolds number
RPM	Revolutions per minute
TGC	Torque generating current (A)
TI	Turbulence intensity (%)
T_F	Frictional torque (Nm)
T_M	Motor torque (Nm)
T_R	Rotor torque (Nm)
TSR	Tip-speed ratio
t	Time (s)
V	Average streamwise flow velocity (m/s)
WC	Wave-current test series
η	Surface elevation (m)
σ_{TI}	Standard deviation turbulence intensity (%)
σ_V	Standard deviation flow velocity (m/s)

1 INTRODUCTION

With a global push towards clean and sustainable electricity production, the marine renewable energy industry has seen increased growth in recent years. Unfortunately, tidal energy technology has not yet reached commercial viability due to high capital and operational costs associated with the challenges of designing, deploying and maintaining turbines in hostile subsea environments. The reliability and durability of devices in these somewhat unpredictable conditions are primary concerns for the industry [1].

Tidal currents vary approximately sinusoidally over time, so the turbine design must take into account the forces associated with the peak current. However, it is most economical to set the peak performance point at a level beneath the maximum current velocity to ensure optimal power capture for a longer portion of the tidal cycle. Variations in the flow speed over shorter time scales will also occur in the field for example due to bed-generated turbulence and ocean waves which can be in the order of 6 s and in a range of 4 to 10 s, respectively [2] [3].

To cope with these continually changing conditions it is desirable for the turbine to be able to shed excess loads (i.e. during peak tidal currents and extreme wave events), to bring the design loads closer in-line with the optimum operational condition. Smoothing of the dynamic loading patterns will also improve the fatigue life of the turbine components and reduce the requirements on the power conditioning system

One way in which this might be accomplished is through the use of passively adaptive (flexible) blades with a built-in coupled bend-twist elastic response under increasing load. This temporarily alters the blade pitch angle, reducing the thrust and torque transferred to the drivetrain, so that excess power is shed once the design conditions are exceeded. The bend-twist mechanism can be manufactured into blades made of composite materials, which are constructed from a number of layers of either woven or unidirectional fibers (i.e. carbon or glass) set in resin. By selecting a suitable orientation of each ply layer in the stack the desired bend-twist response can be achieved ([4], [5]).

There are a number of advantages to this load-shedding solution. Firstly, composite materials are already widely used in the industry to construct rigid blades for prototype tidal turbines. This is due to their high fatigue tolerance, high strength-to-weight ratio, corrosion resistance, and higher damage tolerance compared to commonly used metal materials [6], i.e. composites are well suited to the marine environment [7]. By using this same material, bend-twist blades will retain all of these advantages, without inducing significant alterations to existing manufacturing procedures.

Passive systems have the key advantage of mitigating the need for moving parts (i.e. pitch mechanisms) which are difficult to maintain at sea. Passively adaptive blades should be able to vent the loading peaks dynamically, enabling the design loads for the various turbine components throughout the system to be reduced. This will decrease capital costs, firstly by allowing the technical specifications of the components to be downgraded, and secondly through weight reduction, particularly with regards to the support structure which currently contributes a large percentage of the capital cost [4]. A lower system weight will also lessen the equipment requirements to transport, deploy, and retrieve the device at the tidal site [8].

Ultimately, any perceived benefits of the bend-twist blades must be weighed against any increases in design and manufacturing costs. As the design changes are restricted to re-orientating the angles of the ply layers, it is not envisaged at this stage that this would cause a significant increase in the cost of manufacture or the cost of the blades themselves. In any case, a full economic analysis cannot be completed until the behavior of the bend-twist blades over a full range of hydrodynamic conditions is understood, and their bend-twist response and structural design have been fully optimised for this application.

Investigations into the use of passively adaptive composite blades in the tidal energy industry are ongoing, and previous research has already demonstrated their potential for load regulation in steady

flow conditions. Through towing tank testing of 360 mm long bend-twist composite blades Murray [9] showed that an 11% reduction in the mean thrust loads at design conditions could be achieved. Using a fluid structural interaction (FSI) design tool, verified against the towing tank test results from [9], it was predicted that a 10.4 m diameter full scale turbine with pre-twisted bend-twist blades would have reduced loads and regulated power at flow speeds above design conditions [10]. Nicholls-Lee [11] reported up to a 12% reduction in the thrust loads and up to 5% increase in the power coefficient for an 8 m blade with a bend-twist composite spar using an FSI model. Furthermore, Motley and Barber [12] showed that passively adaptive bend-twist blades could increase annual energy capture by delaying the onset of cavitation, thus enabling the utilisation of larger blades operating at higher rotational speeds [13].

Present understanding of turbine performance in combined wave-current flow is much less comprehensive than that in steady flow. To the authors' knowledge bend-twist blades are yet to be tested in wave-current, and only a small number of researchers have investigated the performance of rigid i.e. non-adaptive blades in these conditions [14], [15], [16], [17], more recently [18], [19], [20] . Importantly, these studies have shown experimentally that wave-current flow can induce significant cyclic variations in the rotor power and thrust at the frequency of the waves. Tatum *et al*. [21] used a computational model to investigate the wave induced variation in bending moments acting at the roots of rigid blades and how these are translated through the drivetrain, causing fluctuating loads on components such as the bearings and seals. Nevalainen *et al*. [22] showed numerically that fluctuating wave loads have the potential to reduce the lifespan of rigid rotor blades and the drivetrain components. Similarly Galloway *et al*. [17] concluded that cyclic loading from waves is likely to result in accelerated fatigue of non-adaptive blades.

The research concerning rigid blades in wave-current flow has revealed significant alterations to the loading patterns, and these dynamic effects are likely to result in more complex interactions with bend-twist blades due to their higher flexibility compared to non-adaptive blades. Moreover, the elastic response and stability of bend-twist blades in dynamic flow conditions will be critical to the blade structural design [23]. With turbine blades having a high risk of failure [24], it is imperative that the blade behavior in these conditions is fully quantified so that it can be appropriately considered in the design process.

As stated previously bend-twist composite blades also have the potential to mitigate the transfer of peak wave loads through the drivetrain, thereby alleviating wear on the turbine components. However, the extent to which the blades can damp the hydrodynamic loading fluctuations is currently uncertain. With this in mind, and considering the prevalence of waves at sites deemed suitable for the installation of tidal energy devices [21], the objective of this work is to investigate experimentally the effects of wave-current loading on bend-twist composite blades.

2 METHODOLOGY

Composite bend-twist and aluminium blades of identical geometry were tested sequentially as part of a three-bladed horizontal axis tidal turbine (HATT) in the wave-current recirculating flume at IFREMER (French Research Institute for Exploitation of the Sea), Boulogne-sur-Mer. The flume specifications are described in [25]. The experiments were conducted at a scale of approximately 1:20, equating to a turbine diameter of 828 mm. In this section the experimental set-up, measurement techniques and test program are described.

2.1 *Experimental setup*

Figure 1 shows the turbine and support structure designed and manufactured at Cardiff University [26]. The turbine stanchion of 71 mm of outside diameter was fixed with two brackets to a steel frame mounted on a crossbeam over the flume at IFREMER. The center of the turbine hub was positioned 1 m below the free water surface and the rotor was operating upstream of the supporting structure, as it can be observed in Figure 1. The flume is 18 m long, 4 m wide and 2 m deep, resulting in a blockage ratio of 6.7% based on the rotor swept area. According to the analysis of [9] this blockage ratio did not warrant the application of any corrections to the data. Furthermore, the study presented in [27] suggests that the turbine's optimum location should follow a submergence of more than half the turbine radius (> 0.5xR) and one turbine radius above the floor (>1xR). In the case of these experiments, both recommendations have been fulfilled by setting the turbine at 2.4xR from the free surface and bottom of the tank. Thus, the size of the flume compared to the rotor also means that the flume walls should not influence the current profile across the rotor swept area. However, the velocity profile is expected to vary with depth once waves are added to the current. This is discussed further in Section 3.

The rotor dimensions and blade geometry are shown in Table 1 and Figure 1. The composite blades were constructed from unidirectional graphite epoxy composite skins with a Sicomin PB 250 closed-cell foam core with a density of 250 kg/m3. The composite skins on the working section of the blades had fibers oriented at 26.8º from the long axis of the blade with a mirrored layup, as detailed in [9], to induce bend-twist coupling. The root section had 6 additional layers of 0.2 mm thick composite with alternating ply angles of 15º and -15º, and a 316 stainless steel cylinder was inserted at the root for added strength. This was extended with a stepped down diameter to connect the blades to the hub (see Figure 1), which was held in place by a 4.5 mm diameter grub screw that slotted into a corresponding notch in the blade root. The mass distribution per section of the composite blades can be found in Table 1.

The aluminium blades were manufactured using a 5-axis CNC machine and based on the measurements obtained from scanning the composite blade with a coordinate measuring machine. The mass distribution of the solid metal blade is also found in Table 1.

The surface roughness of the blades was measured with a Renishaw Equator™ 300 gauging system. The composite blade had a roughness average value of 0.8 ± 0.02 µm compared to an average value of 0.93 ± 0.4 µm measured for the aluminium blade.

Table 1 Geometry of the aluminium and composite blades

Radius (mm)	Blade length (mm)	Blade twist (Deg)	Blade chord (mm)	Aerofoil shape	Blade weight Aluminium (g)	Blade weight Composite (g)
0						
50						
54	4	N/A	15.0	Root insert	-	-
92	42	N/A	29.0	Circular root	-	-
112	62	N/A	N/A	Lofted (ellipse)	-	-
123	73	0.0	64.3	NREL S814	16.9	1.2
137	87	3.0	62.8	NREL S814	21.2	3.2
166	116	8.3	61.0	NREL S814	41.9	4.1
196	146	12.4	59.0	NREL S814	39.7	3.6
225	175	15.4	55.5	NREL S814	34.3	3.1
254	204	17.5	50.9	NREL S814	30.0	3.0
283	233	18.9	46.3	NREL S814	25.9	2.7
312	262	19.8	42.9	NREL S814	22.1	2.4
342	292	20.3	40.6	NREL S814	19.2	1.9
371	321	20.6	37.6	NREL S814	15.1	1.6
400	350	20.9	29.4	NREL S814	13.0	1.3
414	364	21.1	21.3	NREL S814	4.3	0.7
421	371	21.1	13.0	Rounded tip		

The blade root pitch was fixed at the optimum angle for power capture with respect to the chosen blade geometry, at 28.89°. As discussed in Section 1, passive control of excess loads is built into the blades via the bend-twist response, rather than employing an active pitching mechanism to perform this function.

Note that the blade design in [9] focused on creating robust blades for proof of concept laboratory testing. Optimisation of the blade layup to tailor the bend-twist response for the actual design conditions should be conducted once a more complete understanding of the blade behavior has been gained from the scaled experiments, and validated computational models have been developed.

To enable comparison of the bend-twist blades with a set of rigid blades, aluminium blades were manufactured using a 5-axis CNC machine from a CAD drawing based on 3-D scans of the composite blades. Further details of the blade geometry (including pre-twist and chord), as well as the blade design and material properties are given in [9].

For each test condition the turbine was operated at a constant rotational velocity using a Bosch Rexroth motor [28] with a rated power of 0.6 kW, rated torque of 22.5 Nm, and rated speed of 350 RPM. An encoder mounted at the end of the driveshaft monitored the rotational velocity and position, providing dynamic feedback for the motor speed control. The motor and encoder outputs were logged using a National Instruments LabVIEW data acquisition system.

The flow velocity was measured at hub height during the tests using a laser Doppler velocimeter (LDV) located 3.6 m upstream of the rotor. The average resolution was greater than 45 Hz across all test cases. The LDV measurements were initiated by a trigger from the LabVIEW system.

A resistance type wave probe installed on the carriage and positioned in-line with the rotor blades measured the surface elevation during the wave-current tests. Prior to testing, the probe height in still water was adjusted to a number of known positions to convert the output voltage to units of length. The probe was connected directly to the LabVIEW data acquisition system so that its output was synchronised with the other data streams.

To quantify the turbine performance under the applied hydrodynamic loads, the rotor torque (derived from the tangential force component with respect to the rotor plane) and rotor thrust (normal force component with respect to the rotor plane) were monitored.

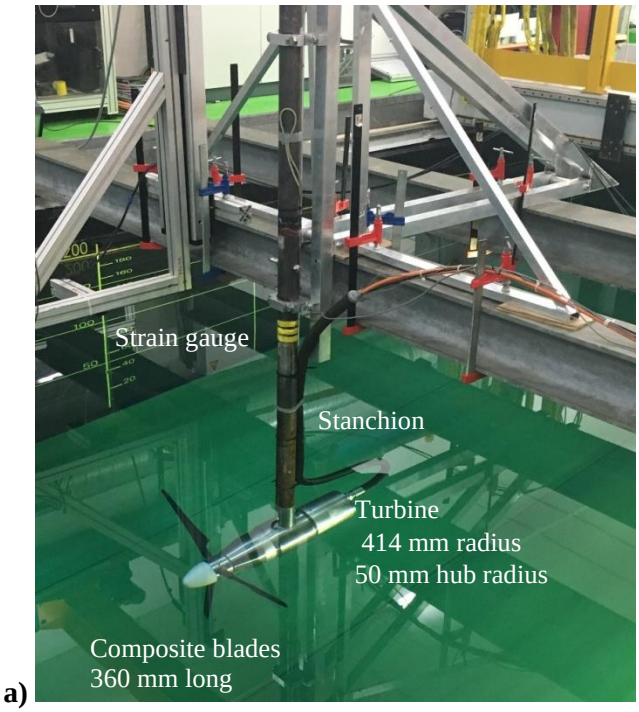

a)

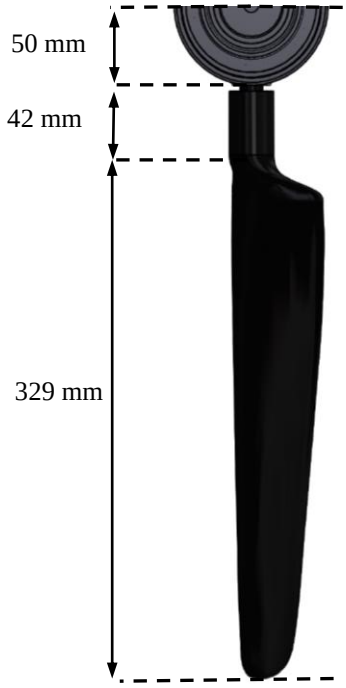

b)

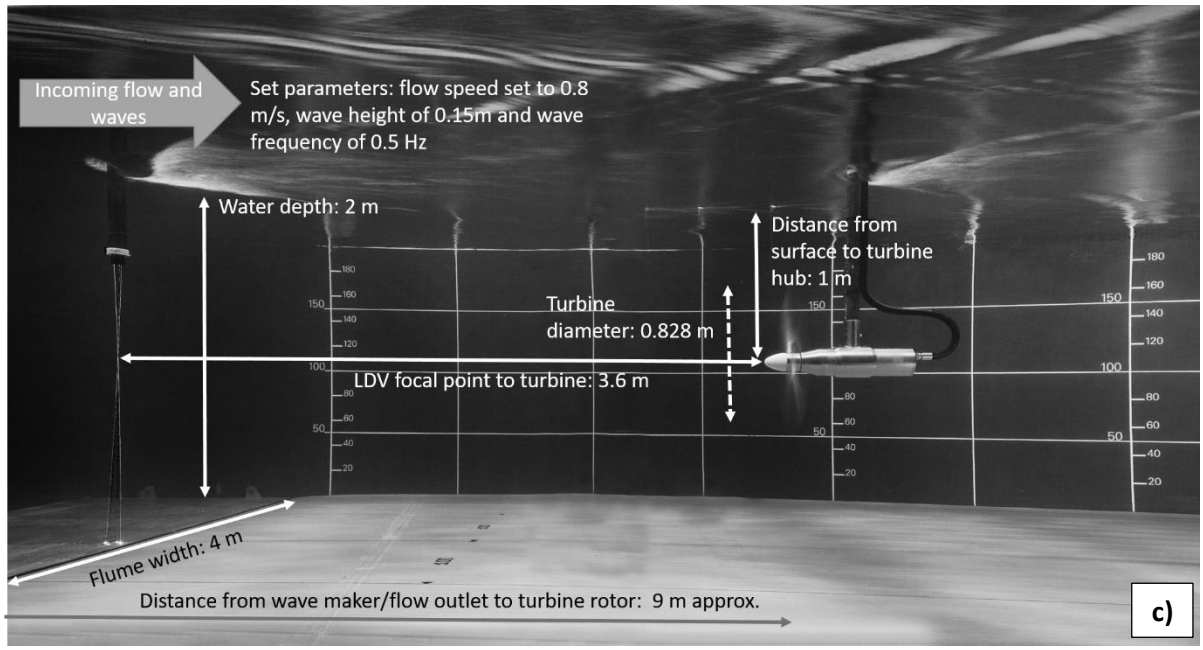

Figure 1 a) Cardiff University turbine with composite bend-twist blades in the wave-current flume at IFREMER, b) Rotor blade and hub dimensions and c) the experimental set-up (photo credit Dr Allan Mason-Jones).

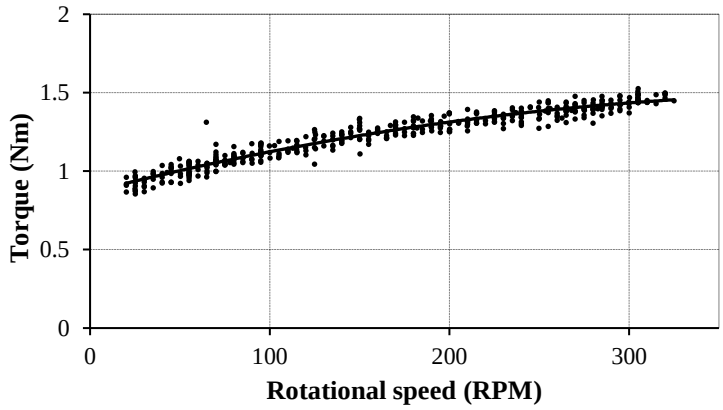

Figure 2 Measured motor torque at different turbine rotational velocities without the blades attached to the hub

The rotor torque was obtained from the motor torque generating current (TGC) recorded in the LabVIEW system at a resolution of 16.67 Hz. The TGC is the electric current required by the motor to drive and maintain the selected turbine rotational velocity. It is related to torque by a torque constant, specified by the manufacturer as 6.66 Nm/A for this motor. The magnitude of the TGC depends on the hydrodynamic torque contribution from the turbine blades, and the friction generated in the drive shaft which varies with the set turbine rotational velocity. To determine this frictional contribution, the motor was calibrated in still water by measuring the TGC without the blades attached to the hub at a range of rotational speeds, see Figure 2. The scatter in the calibration data in Figure 2 is discussed in Appendix 1, and was taken into account when calculating the error bars shown in Section 4. The rotor torque was determined from the measured TGC and the polynomial regression equation for the frictional component (shown in Figure 2) as follows:

$$T_R = T_F - T_M \tag{1}$$

$$T_F = -0.0000034 * RPM^2 + 0.0029101 * RPM + 0.8660455 \tag{2}$$

$$T_M = 6.66 * TGC \tag{3}$$

where T is torque; subscript R denotes the rotor (hydrodynamic) component, subscript F denotes the frictional component and subscript M denotes the motor component.

To measure the rotor thrust the turbine stanchion was instrumented with a 5 mm long, Y11-FA-5-120 strain gauge, with a 119.9 Ohm resistance and 2.01 ± 1% gauge factor, which was located 1.5 m from the turbine hub center (0.5 m above the free water surface), see Figure 1. This was also connected to the LabVIEW data acquisition system and the data was sampled at 250 Hz. The strain gauge was calibrated by measuring the voltage output for a set of known applied loads acting on the hub in the streamwise direction. With the blades removed from the hub, the thrust acting on the stanchion was also measured in a range of flow speeds. The value of the stanchion thrust (without blades attached) at the

appropriate flow velocity was then subtracted from the measured value during testing to obtain the thrust associated with the rotor blades.

2.2 *Test program*

The test program consisted of similar test series for the aluminium and composite blades. Firstly these were conducted under current of constant average velocity, denominated the CO test series. The same current settings were then employed with the wave makers installed in the flume but inactive to check for any influence of their presence on the average current speed and turbulence intensity (CM test series). Finally, the same current settings were applied with the waves switched on, generating co-directional wave-current flow; i.e. the waves were propagating with the current (WC test series). A number of repeat tests were included in the program to enable an uncertainty analysis to be completed (Appendix 1).

Current speeds of 0.8 m/s, 1.0 m/s and 1.2 m/s were employed in the current only (CO) testing. These values were selected based on the scaling considerations, and the limitations of the flume and turbine/blade design. Testing at different flow velocities enables the effect of Reynolds number on the results to be assessed (see Section 4). Although, taking into account the results of previous tow tank experiments and computational model predictions [9], it is anticipated that the influence of Reynolds number will be small over this parameter range.

The rotational speed of the turbine was varied from 45 to 110 RPM, to include tip speed ratios between 2-6 at each current speed. Due to the limitations of the flume facility waves were constrained to a height of approximately 0.15 m in conjunction with a 0.8 m/s current. The wave period was set to 2 s to produce close to the largest wave induced velocities that the wave machine was capable of, to encourage the maximum possible bend-twist response in the composite blades. Using Froude scaling laws these waves would be equivalent to a height of 3 m and a period of 9 s in a water depth of 40 m at the full scale. These wave parameters would be expected to occur at least annually at typical marine energy sites [29].

3 FLOW AND WAVE CHARACTERISTICS

Before examining the measured torque and thrust acting on the turbine (Section 4), it is important to quantify the flow and wave characteristics recorded by the LDV and wave probes. The streamwise flow velocity, V, is presented as the average measured value at the depth of the turbine hub center, and also as the average velocity profile with depth across the turbine diameter. The turbulence in the flow is evaluated in terms of the turbulence intensity parameter, TI, which is defined as the root-mean-square of the turbulent velocity fluctuations divided by the mean velocity of a time series. Note that the phase averaged velocity was used in these calculations for the wave-current tests, so that the sinusoidal variation in the signal due to waves was not counted as turbulence. The water surface elevation measurements during wave-current testing are also discussed in this section in terms of both the time and frequency domains.

Table 2 Measured flow velocity and turbulence intensity averaged across the rotor diameter, and measured in-line with the hub center averaged across all test runs for each flow condition. Standard deviation values given relate to the average velocity and average turbulence intensity between test runs.

Case	*Upstream point measurement*				*Velocity profile (depth averaged across turbine diameter)*	
	V (m/s)	TI (%)	σ_V (m/s)	σ_{TI} (%)	V (m/s)	TI (%)
0.8 m/s CO	0.80	1.85	0.00	0.11	0.81	1.83
0.8 m/s WC	0.79	8.41	0.00	0.74	0.73	10.74
0.8 m/s CM	0.75	8.65	0.01	2.59	0.70	12.87
1 m/s CO	1.00	1.85	0.00	0.04	-	-
1.2 m/s CO	1.20	1.88	0.00	0.06	-	-

In Table 2 the velocity and TI measured at hub height upstream of the rotor are given. These have been averaged across all available test runs for each of the flow conditions. The 1.2 m/s, 1 m/s and 0.8 m/s current only (CO) test series are in close agreement with their design values, with the low standard deviation between tests demonstrating excellent repeatability of the flow conditions. The TI is consistent between the three flow velocities, and at less than 2% is not anticipated to greatly influence the results.

Due to operational constraints of the flume facility where the utilisation of waves was restricted to flow speeds of 0.8 m/s, a full assessment of the flow across the turbine was not undertaken for the studies presented without waves; i.e, 1.0 and 1.2 m/s. This practice was considered acceptable since [14] showed that the variation of the flow across the water column at the Ifremer facility produces uniform and almost unidirectional axial flows with mean vertical velocities close to zero when the wave makers are not operational and not immersed in the flume.

The results for the CM test series (current only but with wave makers sitting in the flume) shown in Table 2 indicate that the presence of the wave maker has affected both the average velocity and turbulence intensity. The wave maker was located downstream of the current inlet, triggering flow disturbances that persisted along the flume. This has resulted in a reduction in the average velocity and an increase in the turbulence intensity compared to the 0.8 m/s CO series which utilised the same current settings but without the wave makers sitting in the flume. Furthermore, the variability in V and TI between individual test runs is more significant in the CM series (see standard deviation, Table 2) signifying that the conditions were less repeatable than in the CO series.

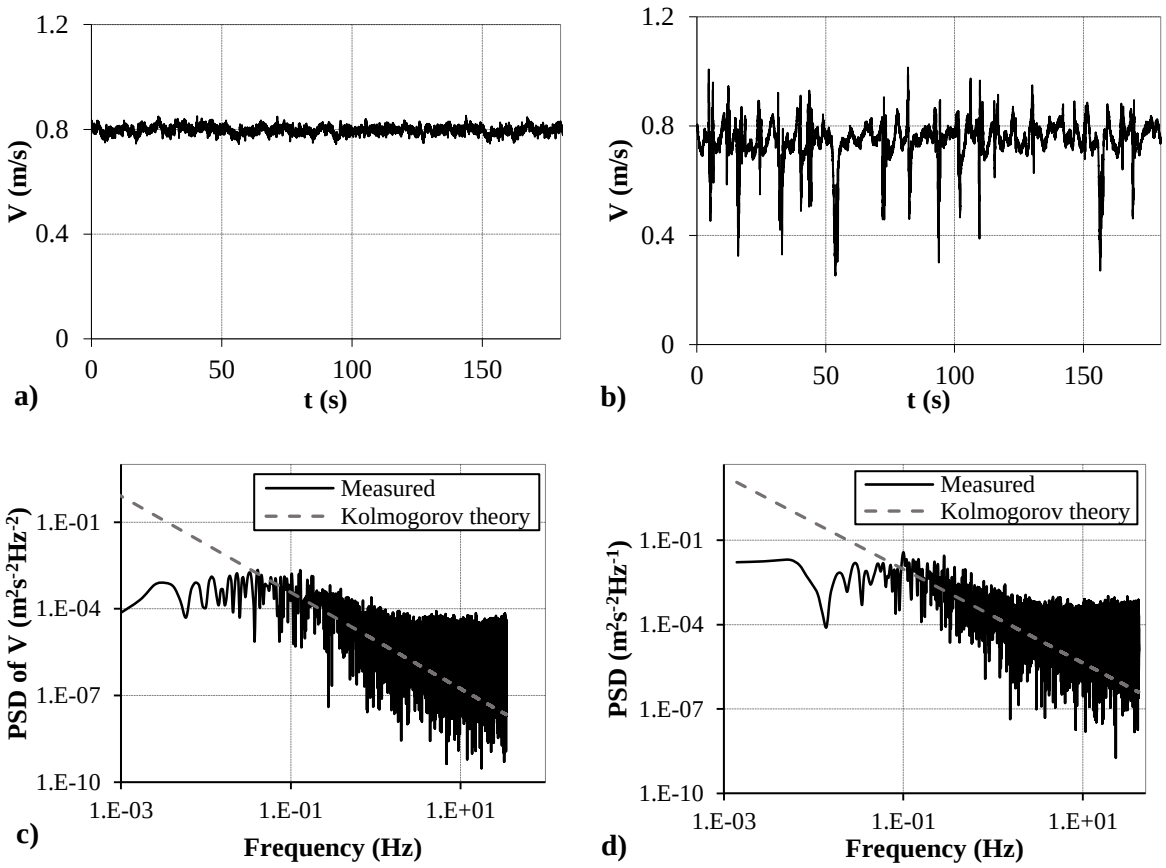

Figure 3 Time histories and power spectral densities of flow velocity measured upstream of turbine in-line with hub center in current with a nominal velocity of 0.8 m/s a) CO series (current alone without wave makers installed in flume) velocity signal, b) CM series (current alone with inactive wave makers installed) velocity signal with inactive wave makers installed c) CO series PSD d) CM series PSD (examples shown are for composite blade tests at 65 rpm (1.08 Hz))

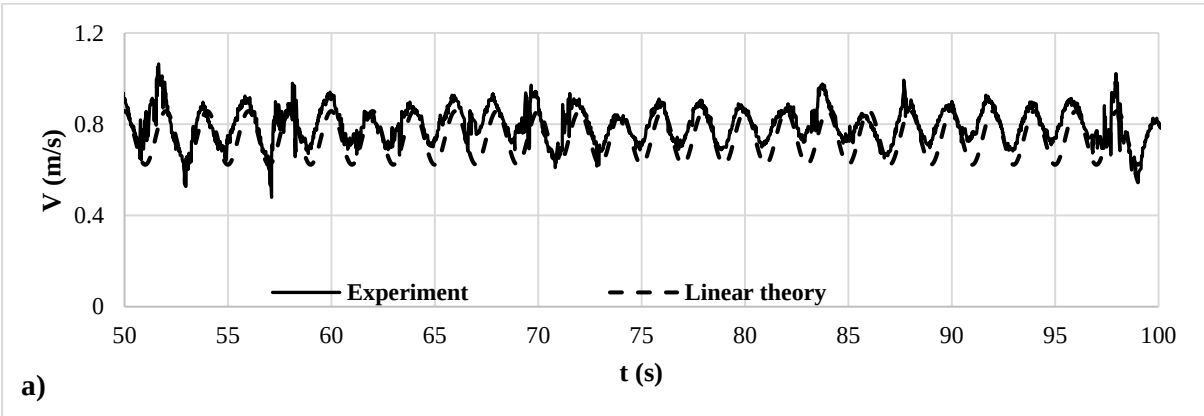

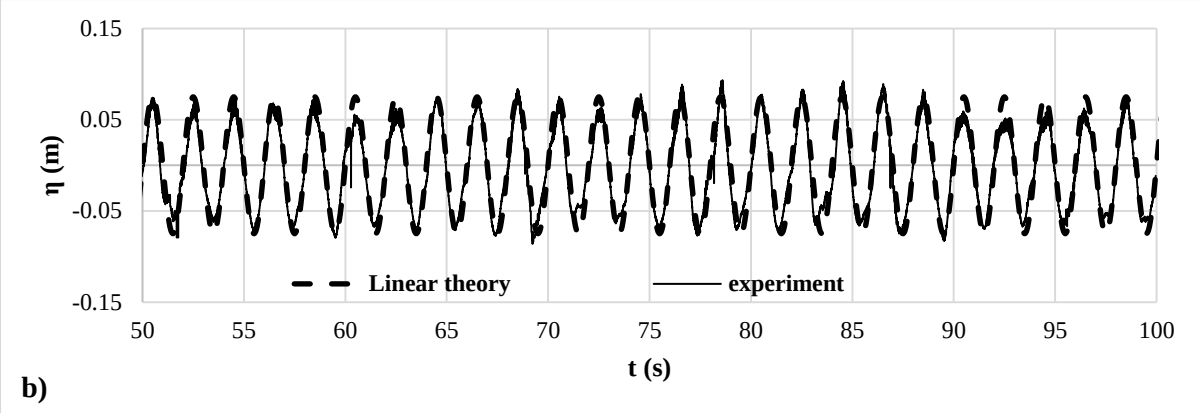

Figure 4 Wave-current flow characteristics a) LDV record of flow velocity at hub height b) wave probe record of surface elevation compared to linear theory (examples shown are for composite blade tests at 65 rpm (1.08 Hz))

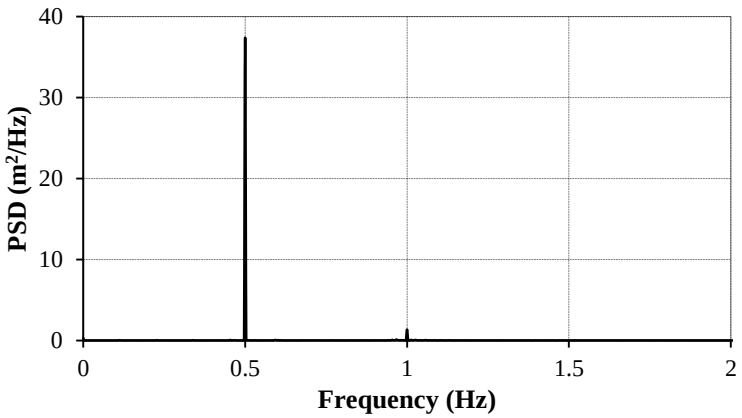

Figure 5 Power spectral density of wave probe record in wave-current flow (composite blade test at 65 rpm (1.08 Hz))

In Figure 3a and 3b typical velocity records from the 0.8 m/s CM and CO test series (current alone with and without the inactive wave makers installed respectively) are compared. The higher level of turbulence due to the wave makers is evident in the CM data (Figure 3b). In Figure 3c and 3d the turbulence spectra are shown for the CO and CM cases respectively. Both demonstrate similar spectra despite the differences in TI. They are broadly in agreement with Kolmogorov turbulence theory, with both cases following the expected -5/3 gradient in the inertial range (Figure 3c and 3d), although there is considerable noise in the spectra at higher frequencies due to the relatively low measurement resolution. Comparison of the tests in these two flow conditions could provide insight into the influence of turbulence on the hydrodynamic loads acting on the turbine. However, the difference in average flow velocity between these two conditions must be taken into account.

In Table 2 the average velocity in the wave-current tests is slightly higher than in the case without waves running (CM series) and the TI is similar. This indicates that direct comparison between the wave-current (WC) and current (CM, i.e. wave maker switched off but still installed in flume) cases is appropriate to discern the effects of wave-current loading on the turbine.

Example time series of the wave-current flow characteristics are presented in Figure 4. The LDV data is shown in Figure 4a and the surface elevation is given in Figure 4b. The 2 s wave period is evident in both data sets. There is notable variation in the amplitude of the velocity fluctuations and wave height, due to the variability in the underlying current as demonstrated when running the current alone (Figure 3b). This level of variability was not present when running the waves alone. While, the wave recreated in the flume corresponds to a 2nd order wave, insignificant non-linearities of the wave mechanics are shown in Figure 4, which compares the surface elevation and the horizontal component of the wave velocity with the superimposed current velocity with predictions obtained from linear theory. The wavelength for this wave characteristics is of 8.3 m.

The average wave height in the combined wave-current flow was approximately 0.15 m. The average horizontal velocity range per wave cycle at hub height across all wave-current tests was 0.31 m/s (39% of the average velocity) with an average maximum velocity per wave cycle of 0.93 m/s and average minimum velocity per wave cycle of 0.63 m/s.

Figure 5 shows the wave probe signal in the frequency domain for a typical wave-current test, establishing the presence of the dominant wave frequency at 0.5 Hz. To a smaller extent the wave harmonics are also present, primarily at twice the wave frequency as a result of wave non-linearity. The presence of these higher frequencies in the waveform is important to note as they may influence the frequency response of the turbine, as discussed in Section 5.

Additional velocity measurements were taken to determine the variation in the streamwise flow velocity with depth through the water column. These were collected once the turbine had been removed from the flume. Figure 6 shows the average velocity profiles recorded in the comparable current alone cases with and without the wave makers installed (CM and CO series respectively) and in the wave-current condition. There is only a small change in the velocity and TI profiles with depth for the current alone case without wave makers installed, indicating that the turbine was situated above the flume bottom boundary layer. The CM series (current alone with inactive wave makers installed) has decreasing velocity and increasing turbulence intensity in the upper section of the profile, coinciding with the draft of the wave maker which spanned the upper part of the water column. The wave-current case (WC series) also has decreasing velocity and increasing turbulence intensity towards the water surface in Figure 6. However, this is to be expected in co-directional wave-current flow, see [30], [31], [32].

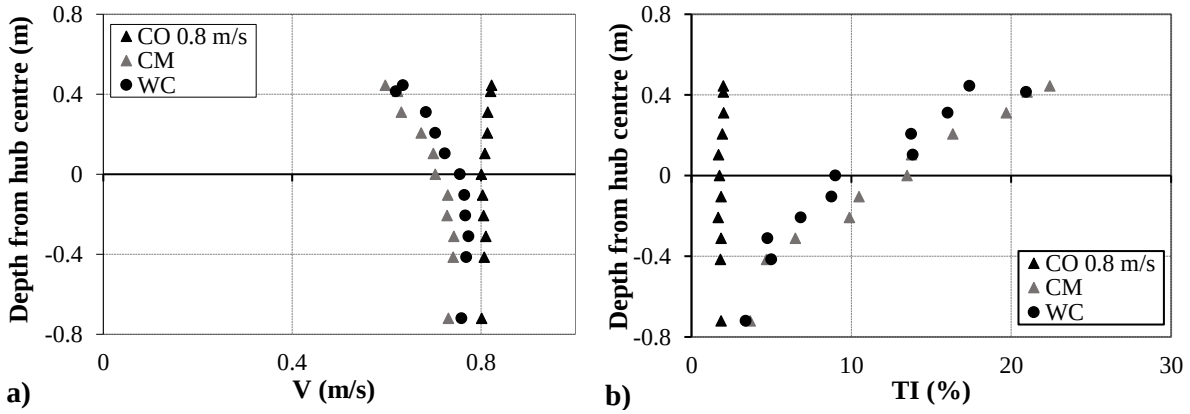

Figure 6 Variation in flow characteristics with depth for the current only cases with and without inactive wave makers installed in the flume (CM and CO series respectively) and the wave-current (WC) test series at a nominal current velocity of 0.8 m/s a) velocity profile b) turbulence intensity

In Table 2 the velocity measured at the hub center and the velocity averaged across the turbine diameter are compared. These are in close agreement for the current alone (CO) case without wave makers installed, as both the velocity and TI were reasonably constant with depth (see Figure 6). For the CM (inactive wave makers installed) and wave-current cases there is a greater difference between the average velocity measured at the turbine centerline compared to that averaged over the rotor diameter, with lower average velocity and higher turbulence intensity when the velocity profile is taken into account. This demonstrates the importance of quantifying the inflow velocity over the full turbine swept area in order to accurately assess turbine performance characteristics. However, in practice this is difficult to achieve during testing without interfering with the experiments, and further consideration of suitable measurement techniques is needed to ensure the necessary information is captured in subsequent laboratory studies. The way in which the velocity is defined will influence the coefficients of power and thrust and this is discussed in terms of the results in Section 4.2.

4 MEAN TURBINE PERFORMANCE CHARACTERISITICS

The average thrust and power measured at each turbine rotational velocity selected for the wave-current (WC) test series and current alone cases with and without inactive wave makers installed (CM and CO series), are shown in Figure 7. For clarity the thrust and power results are presented separately for each blade type. Both the thrust and power increase with flow velocity in Figure 7, and for each flow condition the power and thrust vary similarly with RPM. There is a peak coinciding with the optimal angle of attack, with torque and thrust reducing at slower and faster turbine rotational speeds. The position of the peak moves to the right (higher RPM) at higher flow velocities to maintain the same relative velocity between the turbine and the incoming flow.

The bend-twist behavior of the composite blades can be quantified through comparison with the performance of the aluminium blades. The tests run in the three uniform current (CO) cases, without the wave makers installed in the flume, are considered first in Section 1.1. These results are then

compared with the current alone tests with the inactive wave makers installed in the flume (CM series) in Section 4.2. The wave-current (WC) series is discussed with respect to the CM series in Section 4.3. The error bars shown in Figure 7 and Figure 11 were computed based on the uncertainty in the measurement calibrations, manufacturers' specifications, and repeated test data, as discussed in Appendix 1.

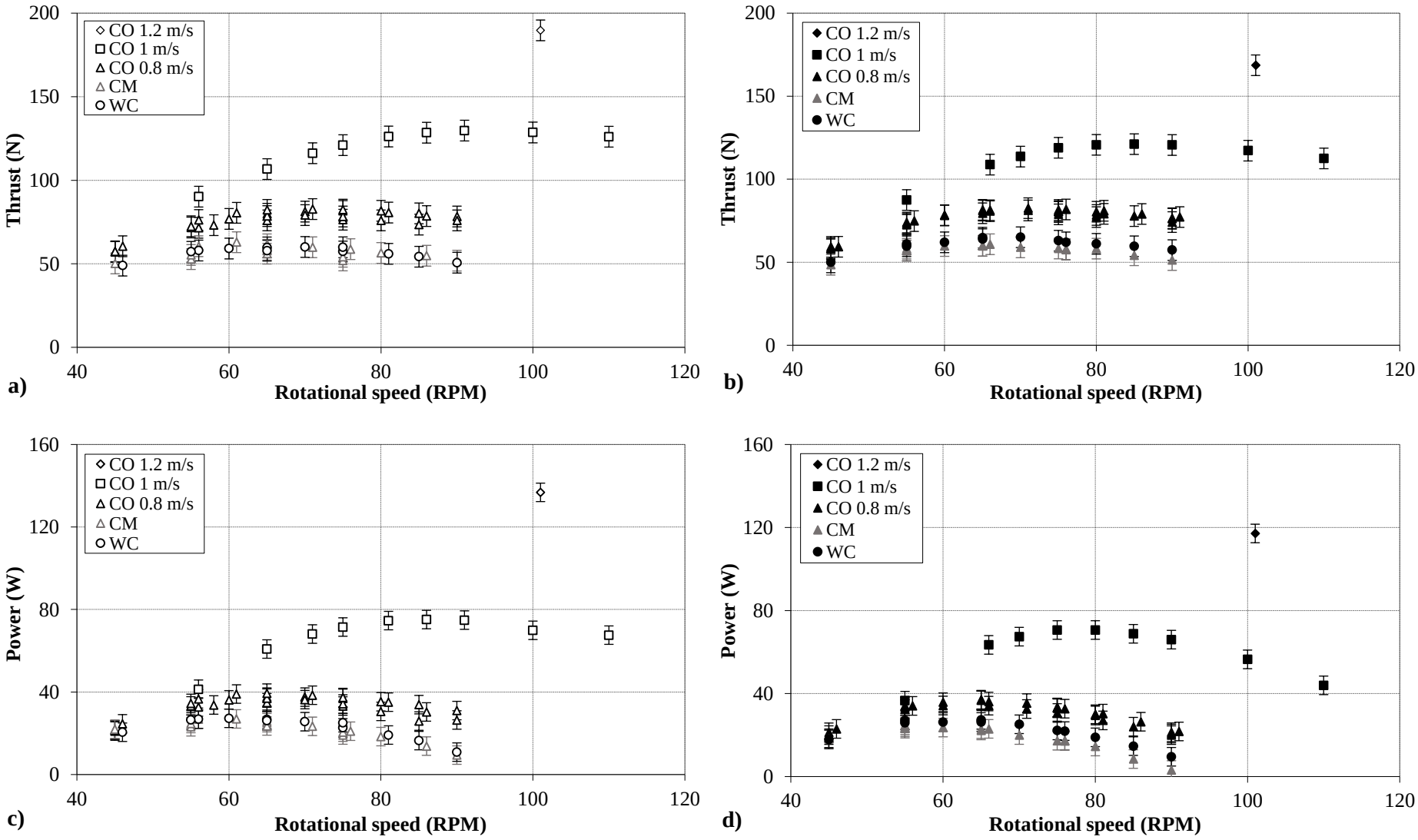

Figure 7 Variation in thrust and power with turbine rotational velocity for each flow condition and blade type a) thrust, aluminium blades b) thrust, composite blades c) power, aluminium blades d) power, composite blades

4.1 *Uniform current tests (CO series)*

The performance characteristics of the composite and aluminium blades are compared in Figure 8 and Figure 9 for the current only (CO) test conditions (i.e. without wave makers present in the flume). The data is presented in the form of the thrust and power coefficients, C_T and C_P, as a function of the tip speed ratio, TSR. These parameters represent the actual rotor thrust, power and rotational velocity normalised by the available thrust, power and free-stream velocity, as detailed in [33]. Non-dimensionalising the parameters in this way facilitates direct comparison of the data collected under the different flow velocities.

The C_T values for the aluminium and composite blade tests in 0.8 m/s current are shown in Figure 8a. While there is scatter in the data, the polynomial regression lines are in close agreement and the error bars overlap (Figure 7), indicating that the magnitude of the thrust acting on the composite and aluminium blades is similar.

In Figure 8b the C_T values for the aluminium and composite blade tests conducted at the 1 m/s and 1.2 m/s current velocities are compared. There is a noticeable difference in the loads on the two blade types at higher TSR values, with a reduction in thrust on the composite blades. This is not evident in the 1 m/s current tests at lower TSR values (i.e. lower RPM) where the curves for the two blades are in close agreement. At the 1.2 m/s current velocity the reduction in thrust associated with the composite blades is greater compared to that in the 1 m/s set at the same TSR value, indicating that the magnitude of the thrust reduction increases with flow velocity. The maximum reduction in C_T is approximately 11%, which is in close agreement with the results of Murray *et al*. [34], providing confidence in the test methodology. This indicates that, at least in this context, the 2% difference in TI between the present study and that of [34] has not affected the behavior of the blades in this respect; however higher turbulence intensities may affect the operation of devices considerably, as shown in [35]. These results have also been replicated to a reasonable degree by the two-way coupled BEMT-FEM computational model in [34].

Similarly to the C_T data, the C_P values for the two blade types, shown in Figure 9, are in close agreement at lower TSR values. The C_P measurements for the composite blades then begin to reduce compared to those for the aluminium blades as TSR and flow velocity increase. This amounts to a significant reduction in C_P at the highest TSR values tested (35% reduction in the 1 m/s case). The peak value of C_P is also reduced due to the composite blades, by nearly 7% for the 1 m/s case and by approximately 14% in the 1.2 m/s case. Even at the lowest flow speed of 0.8 m/s there is a small reduction of 3% at peak power which increases to a notable 26% at the maximum TSR value. While passive power reduction is beneficial above rated conditions, these results demonstrate the need for careful design of bend-twist blades so that power capture is not diminished during normal operating conditions. As mentioned in Section 2 the primary design objective for the blades at this stage was to demonstrate the

potential of the concept, rather than attempting to hone the bend-twist response to generate optimal performance curves. Therefore, these results are encouraging because they show, as hypothesised, that both the thrust and power transmitted to the turbine can be reduced passively by the bend-twist blades.

The differences between the aluminium and composite blades in terms of both thrust and power are more significant at higher values of RPM and flow velocity because as these parameters increase, so will the forces acting on the blades. This will cause a greater degree of bend-twist in the composite blades, shedding more power and thrust relative to the characteristics of the aluminium blades. At the lowest flow velocity and turbine rotational velocities tested the forces are small enough not to induce a significant bend-twist response in the composite blades, hence the loads on the composite and aluminium blades are similar under these conditions.

When comparing the results for the aluminium blades in Figure 8 and Figure 9 at the three current velocities, there is only a small increase in the peak C_P and peak C_T values with increasing flow velocity. As the data has been normalised, this implies that the influence of Reynolds number (Re) is small over this range. The critical Reynolds number to achieve Reynolds independence (based on the turbine diameter) was found by Mason-Jones [36] to be 5×10^5, and the effect of Reynolds number was insignificant for $Re>2x10^5$. The Reynolds number for the turbine in the present study at a current speed of 0.8 m/s and similar to Mason-Jones [36] based on the turbine diameter, is 6.6×10^5. While a different blade geometry was used in the present study to that in [36], this should not affect the critical Reynolds number at least in terms of its order of magnitude. Therefore, the test conditions in the present study are thought to be approaching independence.

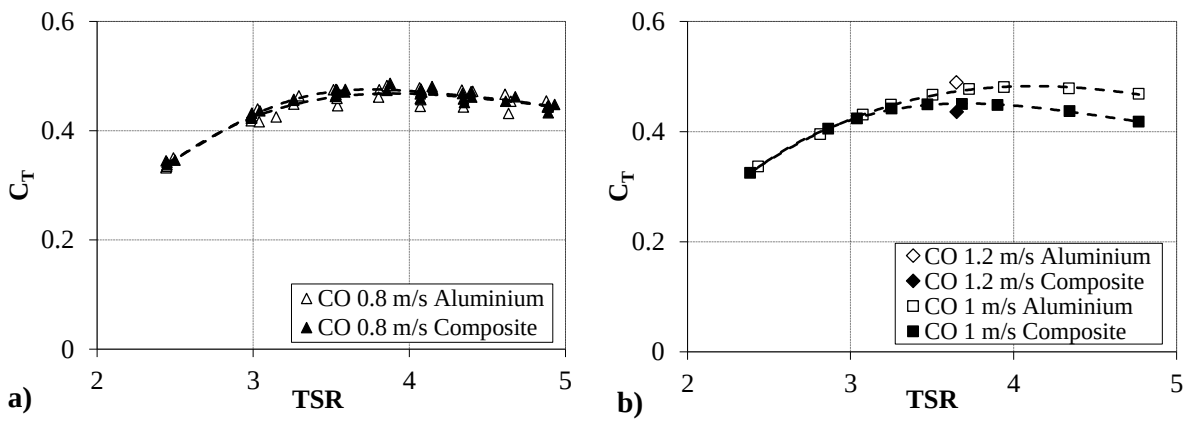

Figure 8 Comparison of variation in the thrust coefficient with tip speed ratio for the two blade types, current only (CO) test series, without wave makers installed a) 0.8 m/s b) 1 m/s and 1.2 m/s. Polynomial regression lines for each data set are shown to aid comparison.

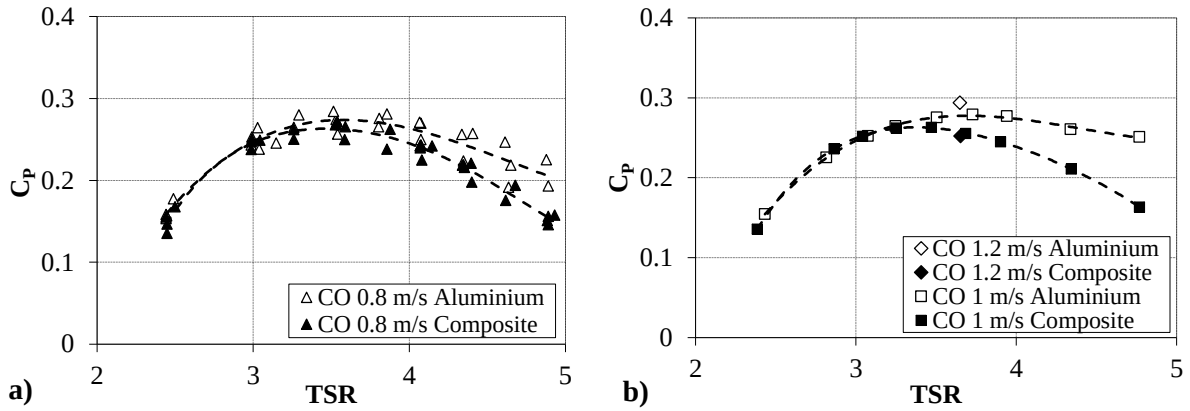

Figure 9 Comparison of variation in the power coefficient with tip speed ratio for the two blade types, current only (CO) test series, without wave makers installed a) 0.8 m/s b) 1 m/s and 1.2m/s. Polynomial regression lines are shown for each data set to aid comparison.

4.2 *Comparison of current tests at a nominal velocity of 0.8 m/s (CO and CM series)*

In Section 3 it was found that in the current alone (CM) series with inactive wave makers installed in the flume the presence of the wave makers altered the characteristics of the current, reducing the average velocity and increasing the turbulence intensity. It is interesting to consider the effect of this on the turbine performance.

As shown in Figure 7, the lower average velocity (and possibly the increased turbulence intensity) in the CM condition with inactive wave makers installed has resulted in a reduction in both thrust and power compared to the same blade type in the 0.8 m/s CO test series without the wave makers present. The peak thrust and peak power have been reduced by approximately 26% and 28% respectively.

To understand the influence of turbulence, first the effect of the difference in average velocity must be removed, by plotting the data in non-dimensional form. In Figure 10 this is done using two different definitions for velocity. In Figure 10a and 10b the coefficients of thrust and torque plotted against the tip speed ratio were computed using the average velocity measured at hub depth during each test run. In Figure 10c and 10d the velocity profiles measured after testing are utilised to estimate the average velocity across the rotor swept area, following the method of [37]. Note that this velocity parameter is very similar to the depth averaged velocity across the rotor diameter in this study as velocity measurements were not collected in the cross-stream direction due to time constraints. By taking into account the velocity across the full rotor swept area close agreement is achieved between the curves for the two blade types (Figure 10c and 10d), despite the increased scatter due to these measurements not being related to specific test runs. Whereas, using the point measurements of velocity the coefficients of thrust and torque are smaller in the CM test series (Figure 10a and b).

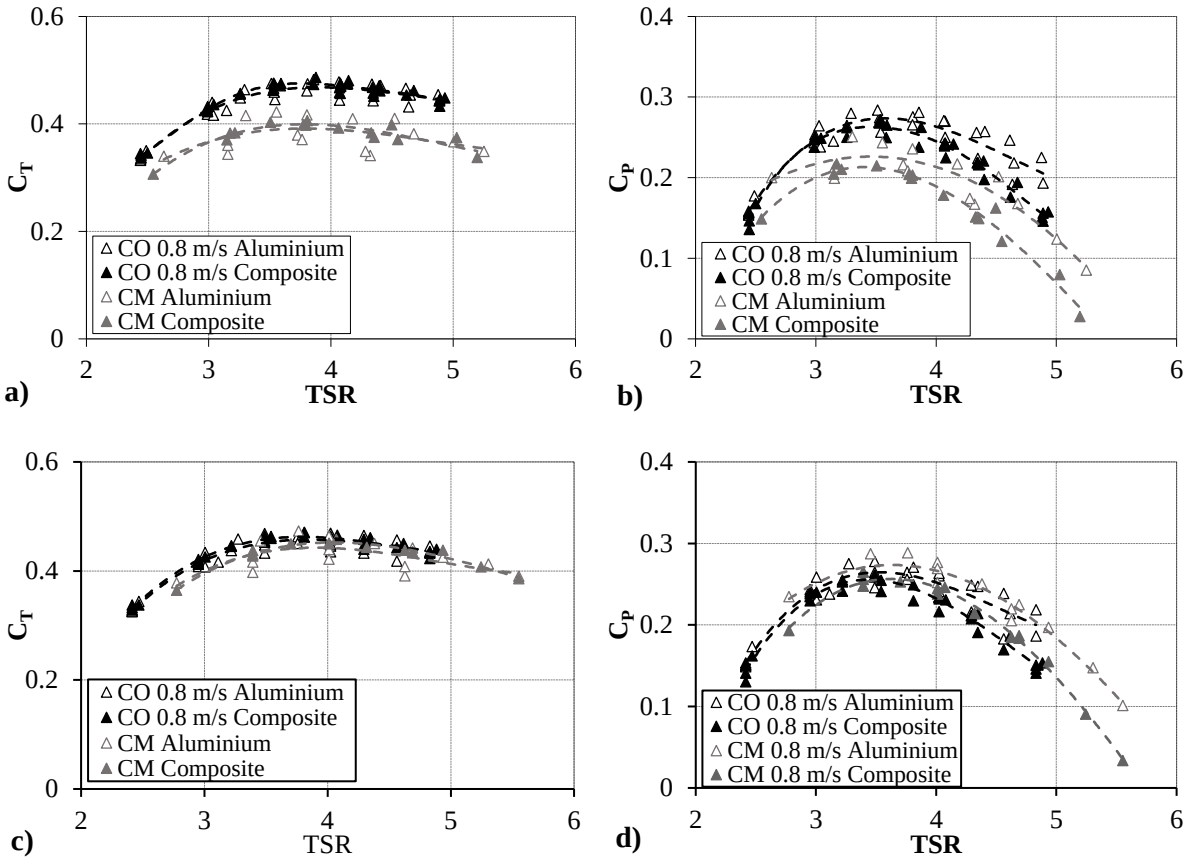

Figure 10 Comparison of turbine performance in the CM and CO test series with and without inactive wave makers installed at a nominal velocity of 0.8 m/s, aluminium and composite blades a) thrust coefficient using point measurement velocity for each test b) power coefficient using point measurement velocity for each test c) thrust coefficient calculated from estimate of velocity averaged over turbine area from velocity profiles, Figure d) power coefficient calculated from estimate of velocity averaged over turbine area from velocity profiles. Polynomial regression lines are shown for each data set to aid comparison.

The Reynolds number based on the average velocity for the CM condition is still above the critical Reynolds number defined by [36]. Therefore, it is likely that the influence of Reynolds number is small, and hence agreement between the CO and CM cases is to be expected, as in Figures 10c and 10d. This implies that the increased turbulence intensity (Table 2) once the wave makers were installed in the flume (CM series) has had little effect on the average values of either C_P or C_T.

In Figure 7 the thrust and power curves for the two blade types are similar for the CM case with inactive wave makers installed in the flume, and are within the measurement uncertainty. When plotting this data in terms of the coefficients of thrust and torque in Figures 10c and 10d, there is also little difference between the coefficient of thrust for the two blade types. For the coefficient of power, Figure 10d, the expected trend of reduced C_P in the composite blades at higher tip speed ratios is somewhat evident. Nonetheless, the results indicate that, as with the 0.8 m/s CO test series, the forces associated with the CM flow condition are not substantial enough to produce a considerable bend-twist response in the composite blades.

4.3 *Comparison of current and wave-current tests (CM and WC series)*

The aluminium and composite blade behaviors in the wave-current condition are presented in terms of average thrust and torque in Figure 11. The results from the current alone case with wave makers present but inactive (CM series) are also included in Figure 11 for comparison. For the aluminium blades the wave-current (WC) and current (CM) cases are in close agreement, indicating that the average forces in wave-current and current are similar, as has been reported previously by [14] and [18].

For the composite blades both the power and thrust are a little higher in the wave-current (WC) series compared to in the current (CM) tests. However, these differences are still within the measurement uncertainty based on the repeated tests (see Appendix 1), and so without conducting further testing it is not possible to conclude that this is a significant result.

When comparing the wave-current results between the two blade types for both thrust and power these are also within the measurement uncertainty of the instrumentation. As with the tests in current (0.8 m/s CO and CM series) this indicates that the flow velocity is too low to induce much bend-twist in the composite blades, at least in terms of affecting the average loads. This does not mean that the bend-twist blades do not respond dynamically to the fluctuating loads, and this is discussed in terms of the frequency and time domains in the following section.

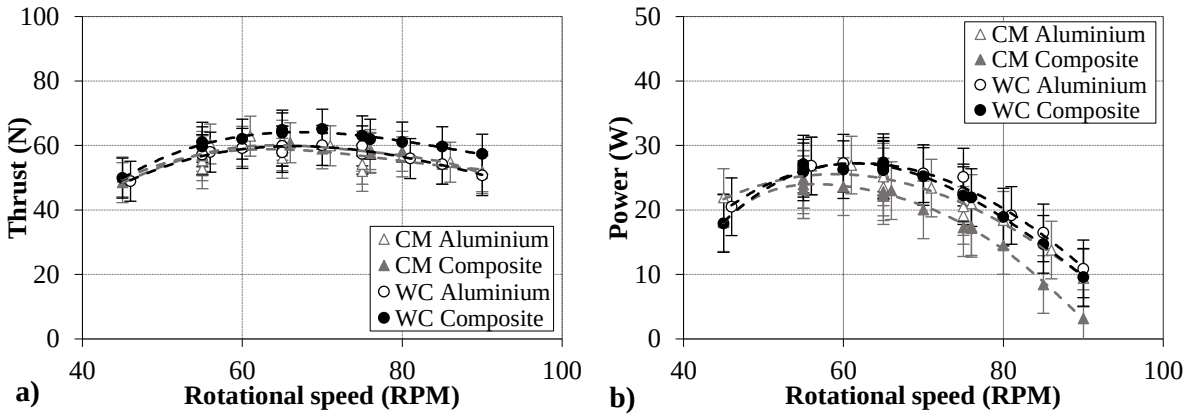

Figure 11 Comparison of variation in power and thrust with turbine rotational velocity for the current alone (CM) and wave-current (WC) test series and both blade types a) thrust b) power. Polynomial regression lines are shown for each data set to aid comparison.

5 FREQUENCY DOMAIN ANALYSIS

Further insight can be gained into the turbine loads by analysing the results in the frequency domain. This allows the amplitudes of vibrations induced in the turbine system at different frequencies to be quantified. These may be due to fluctuations in the incoming flow (turbulence or waves), or related to the rotational period of the turbine and interaction with the support structure.

5.1 *Uniform current tests (CO series)*

Figure 12 shows the spectral analyses, determined by fast Fourier transform (FFT), of the thrust and torque time series for both the composite and aluminium blades operating at optimum RPM in the 0.8 m/s current tests without the wave makers installed (CO series).

In terms of the thrust (Figure 12a) both blade types have similar spectra, with the most prominent frequency being equal to the rotational frequency of the rotor, at approximately 1.1 Hz (65 RPM) for the test case shown. There is also a smaller peak in the spectrum at three times the turbine rotational frequency which corresponds with the rate of the blades passing the stanchion. At this frequency the amplitude is slightly larger for the composite blades, implying they may be bending a little due to interaction with the tower. However, the magnitude of this fluctuation is small enough so as not to induce any change in torque (Figure 12b), and much lower than that at the rotor rotational frequency. Tower interactions were expected to be limited due to the fairly substantial distance between the rotor head and stanchion in the streamwise direction. The higher frequency peak at approximately 5.4 Hz is probably related to the natural frequency of the support structure and mounting frame.

The amplitude of the fluctuations in the torque spectrum are an order of magnitude smaller than those in the thrust spectrum (Figure 12b). The frequencies associated with the turbine rotational period and the stanchion passing frequency are not distinguishable from the background noise associated with the measurement system. Vibrations due to the mounting structure may be more evident in the thrust spectrum because the thrust gauge was mounted directly on the stanchion, whereas the torque was monitored at the motor which was mounted behind a radial shaft seal and a single set of bearings. These drive shaft components are likely to have added damping to the system reducing the level of torsional fluctuations observed in these measurements.

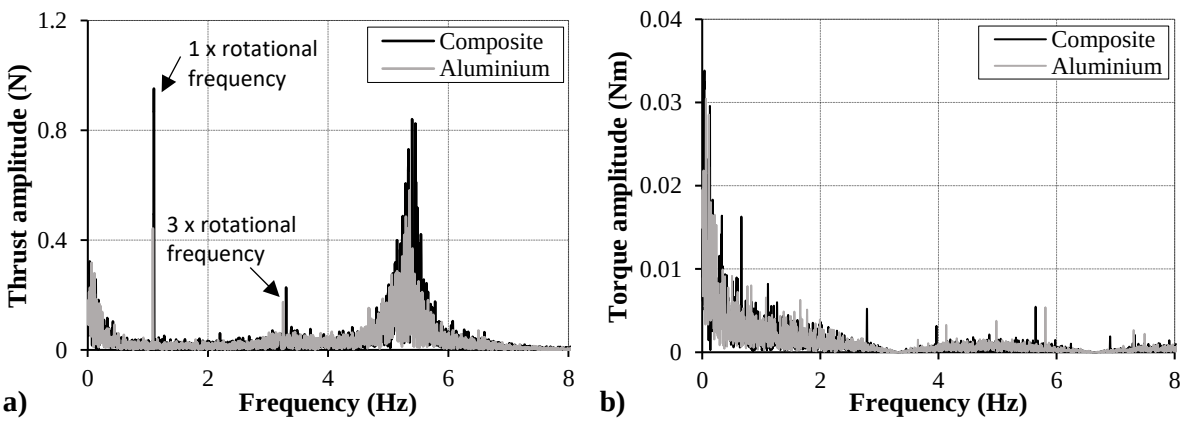

Figure 12 Comparison of the frequency spectra for the aluminium and composite blades, CO test series (current, no wave makers in flume) a) thrust b) torque (examples shown are from 0.8 m/s tests run at 65 rpm (1.08 Hz))

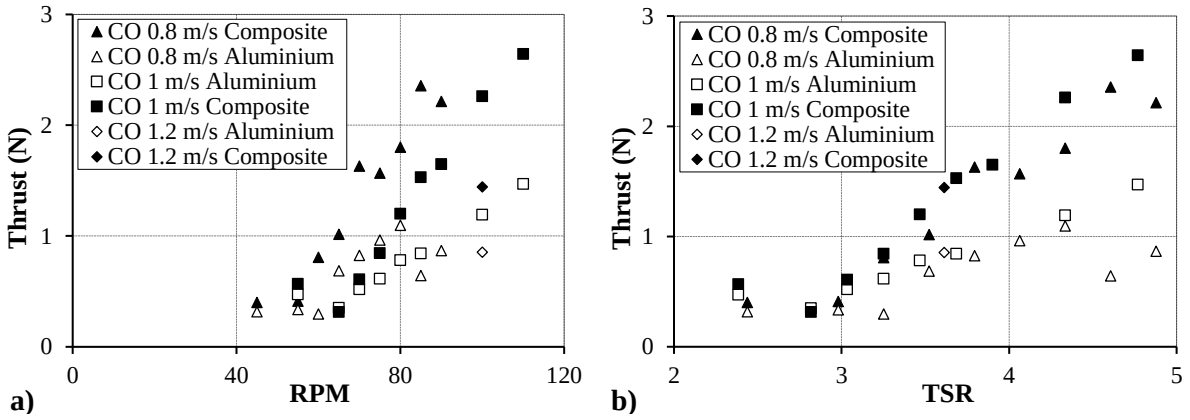

Figure 13 Comparison of the amplitude of the peak in the frequency spectrum at the turbine rotational velocity for the composite and aluminium blades, current only (CO) test series without wave makers installed a) thrust amplitude versus turbine rotational speed b) thrust amplitude versus tip speed ratio

Any fluctuations in thrust and torque associated with the rotor blades should appear primarily at three times the turbine rotational frequency due to superposition of the responses of the three blades. In practice, however, fluctuations at the rotational frequency may occur due to small differences in the blade pitch settings, their geometry, weight or ply lay-up (when considering the composite blades). Fluctuations at this frequency may also be generated by the motor/control system or a small misalignment in the drivetrain.

In Figure 13 the amplitude of the peak in the thrust spectrum at the turbine rotational velocity for each test in the current only (CO) series without wave makers present is shown. The magnitude of the thrust vibration increases with RPM and decreases with increasing flow velocity (Figure 13a). The effect of flow velocity is removed in Figure 13b, although with some scatter, by presenting the results in terms of TSR.

The amplitude of the thrust is higher for the composite blades than for the aluminium blades in Figure 13. This is in agreement with the results of [34]. The difference in blade weights was smaller between the three composite blades (±0.2%) than between the three aluminium blades (±0.9%), so this can be ruled out as the cause. Significant differences in pitch are also unlikely due to the locking mechanism employed. A small difference in deflection between one of the composite blades and the other two blades was identified from static loading tests in [10], probably resulting from differences in the ply layup during manufacture. This may account for the increased fluctuation size at this frequency. Alternatively the higher fluctuations could be a result of vibrations set up by the motor/drivetrain being transferred more so to the composite blades due to their increased flexibility.

While the frequency response in this study is specific to the scaled drivetrain design, at full scale it is possible that vibrations could be induced in flexible blades by the response of other components in the drivetrain or the support structure. Therefore, this is important to consider in the structural design and assessment of the fatigue life of composite blades. However, it should be noted that the actual variations

in thrust (< 3 N) are small relative to the average values of thrust shown in Figure 7 (50-200 N depending on flow speed and RPM), and so would not be expected to be of major concern.

5.2 *Current tests with wave maker installed in flume (CM series)*

Figure 14 shows the thrust and torque frequency spectra for the optimum case in the current alone (CM) test series with inactive wave makers installed in the flume. As with the CO case of current alone without wave makers in the flume (Figure 12), there are peaks in the thrust spectrum associated with the rotational frequency of the rotor and the natural frequency of the mounting system. However, it is difficult to distinguish a peak at the blade passing frequency. This is due to the greater level of noise in the spectrum which is probably related to the higher turbulence in the CM condition. The amplitude of noise in both the thrust and torque spectra is an order of magnitude greater than in the CO case. Similarly to the CO case, the peaks associated with the turbine rotational period and blade passing frequency are indiscernible in the torque spectrum (Figure 14b).

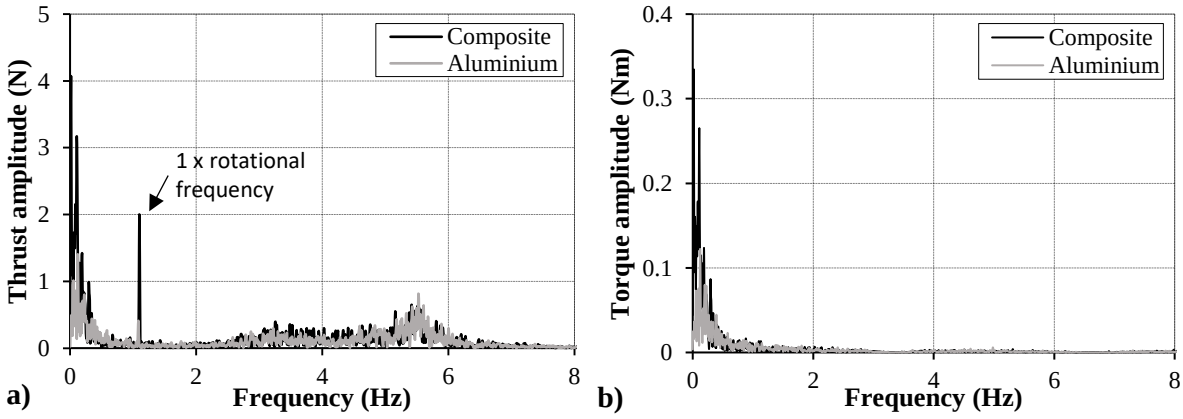

Figure 14 Comparison of the frequency spectra for the aluminium and composite blades, CM test series a) thrust b) torque (examples shown are from tests run at 65 rpm (1.08 Hz) and a flow velocity of 0.8 m/s)

5.3 *Wave-current tests (WC series)*

Figure 15 shows the spectral analyses of the thrust and torque time series for both the composite and aluminium blades for the optimum case in wave-current flow. The dominant frequency in the thrust spectrum (Figure 15a) correlates to the wave frequency of 0.5 Hz. While significantly smaller in magnitude, the rotational period of the turbine is also clearly defined with a peak of similar amplitude to that in the CM case (wave makers inactive, Figure 14a). The amplitude associated with this frequency is slightly larger for the composite compared to aluminium blades, for the same reasons as discussed in terms of the CO tests in Section 5.1. As with the CM case the contribution that relates to the blades passing the stanchion at three times the turbine rotational frequency is not visible in Figure 15a. The natural frequency of the stanchion is present at around 5.4 Hz as in the CM and CO cases.

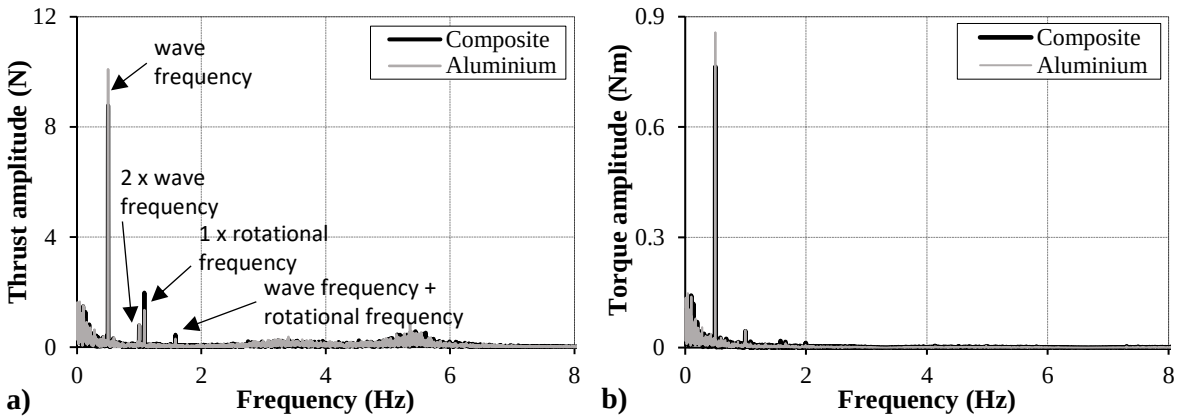

Figure 15 Comparison of the frequency spectra for the aluminium and composite blades, wave-current (WC) test series a) thrust b) torque (examples shown are from tests run at 65 rpm (1.08 Hz) and a flow velocity of 0.8 m/s)

There is a small peak in the thrust spectrum at twice the wave frequency which is linked to the presence of this harmonic in the wave signal, see Figure 5a. The wave frequency and its first harmonic are evident similarly in the torque spectrum (Figure 15b). There is also a small peak at 1.58 Hz in the thrust, and to a lesser extent in the torque spectrum which is equal to the sum of the wave frequency and the turbine rotational frequency. This superposition indicates an interaction effect between the turbine rotational period and the wave period, which was demonstrated and discussed with respect to the loads on a single blade in [38]. Seeing some interaction in terms of the response of the full rotor is interesting as it indicates that the individual blade interactions do not fully cancel each other out in this respect.

In Figure 16 the amplitude of the fluctuations in thrust and torque at the wave frequency are shown for the two blade types for each of the wave-current tests. The amplitude of both the thrust and torque is consistently larger for the aluminium blades than for the composite blades, revealing that the composite blades damp out the oscillatory forces generated by the waves. Significantly, this will moderate the loading fluctuations that are transferred to the drivetrain components at this frequency, thereby reducing their likelihood of failure.

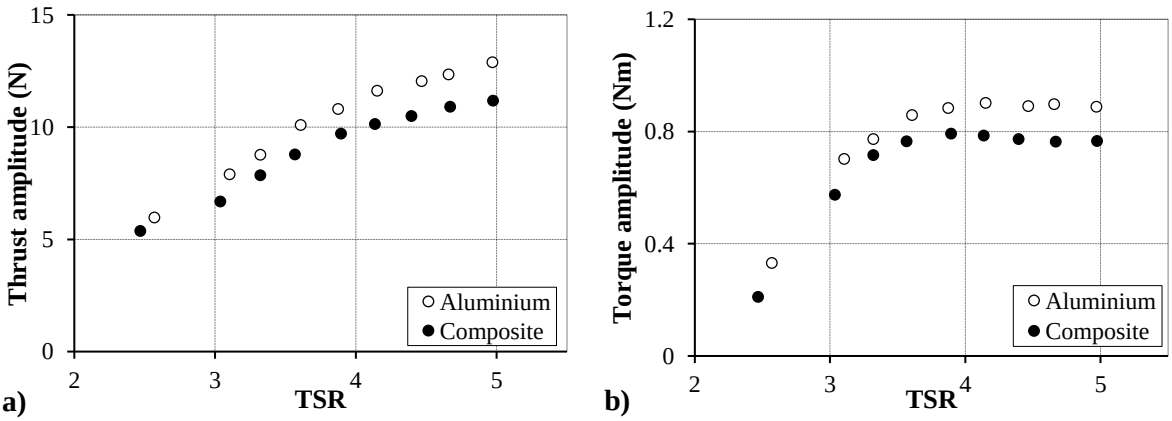

Figure 16 Comparison of the amplitude of the peak in the frequency spectrum at the wave frequency for the composite and aluminium blades in the wave-current (WC) test series a) thrust b) torque

6 TIME DOMAIN ANALYSIS

To quantify the size of the fluctuations in thrust and torque and the damping associated with the composite blades under wave-current loading, the results are investigated in the time domain where the contributions from all of the frequencies discussed in Section 5.3 are combined. Figure 17 shows the average range in thrust and torque per wave cycle.

The magnitude of both the thrust and torque fluctuations are reduced for the composite blades compared to the aluminium blades in Figure 17, corresponding with the results associated with the dominant wave frequency in Section 5.3. The composite blades reduce the size of the thrust fluctuations by up to 10% and the torque fluctuations by up to 14%. The fluctuating forces due to the waves result in increased bend-twist being induced during part of the wave cycle, shedding peak thrust and power.The size of the thrust and power fluctuations for the aluminium blades and the level of damping by the composite blades increases with the rotational speed of the turbine, due to the larger forces induced at higher RPMs, and consequently the greater bend-twist response of the composite blades.

The low flow velocity and relatively small wave height set for the wave-current condition mean that the bend-twist response in the composite blades was fairly limited. If the size of the waves or the current speed was increased, it is likely that the damping of the fluctuating forces would be much more significant, and the average values of thrust and power may also be affected. Moreover, it has been demonstrated by [9] that ideal pre-twisting conditions can be obtained iteratively to produce coupled BT blades that will provide thrust loads reductions close to 9% with power losses of only 5%. Thus, these BT blades can be designed according to the set specifications.

The application of load shedding techniques to the offshore industry provides beneficial properties to the structures such as the reduction of stress range and intensity on a particular area allowing the interruption of crack propagation. However, it has also been noted that greater stresses may be produced elsewhere causing additional damage it [39] [40]. These effects should then be properly studied in the marine renewable energy sector as fatigue failure is not only related to the lowering of load, it is also (and probably more) related to the number of load cycles that these structure are exposed to along with the strain range of the material. It should be noted therefore that further investigations are required to investigate low frequency cyclic loading such as tidal loading (diurnal, semi-diurnal and mixed) and higher frequencies from turbulence, velocity profile and blade support structure interaction along with wave-current interaction exposure. Therefore, this is an area for further work, the first stage of which would be to conduct tests in a facility where wave-current combinations with higher average velocity and larger velocity fluctuations can be tested, i.e. higher current speed, longer wave period and larger wave height, to gain greater insight into the bend-twist blade behavior and support optimisation of the bend-twist blade structural design.

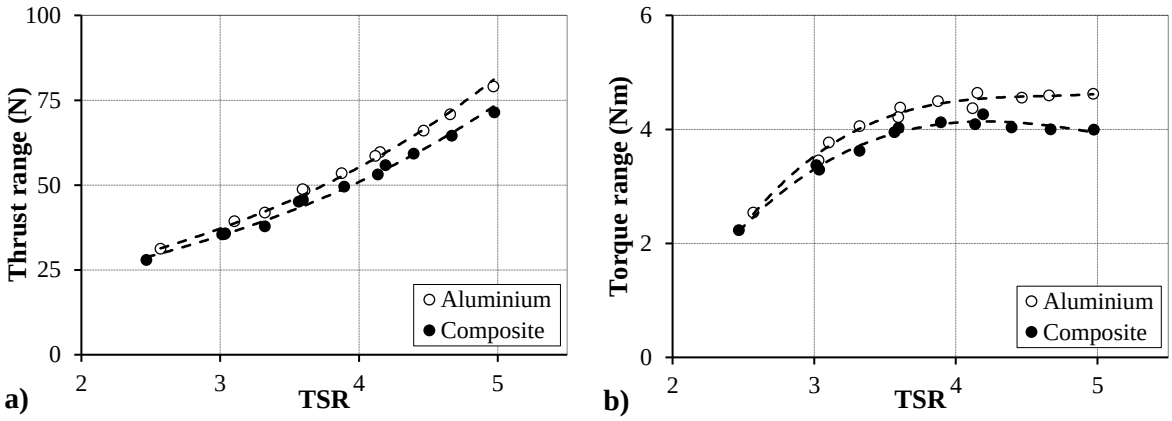

Figure 17 Magnitude of average maximum minus minimum load per wave cycle in wave-current (WC) test series a) thrust range per wave cycle for composite and aluminium blades b) torque range per wave cycle for composite and aluminium blades

7 CONCLUSIONS

The aim of this study was to investigate experimentally the performance of a 1:20 scaled three bladed horizontal axis tidal turbine under current and co-directional wave-current conditions. The turbine was tested with composite bend-twist coupled blades and rigid aluminium blades to characterise, through comparison, the bend-twist response in these flow conditions. The turbine thrust and power were considered as time-averaged quantities and by analysing the dynamic behavior of the turbine in the frequency and time domains.

The main conclusions are as follows:

- Considering the time-averaged data, in uniform current (CO test series) the peak value of C_T was reduced by up to 10% and the peak C_P was reduced by up to 14% due to load shedding caused by the bend-twist response of the composite blades compared to the aluminium blades.
- The size of this load reduction increased with TSR i.e. with flow velocity and with turbine rotational velocity as both of these increased the magnitude of the forces acting on the blades, thereby inducing greater bend-twist in the composite blades. Consequently at the slowest flow velocity and turbine rotational speeds tested the loads on the two blade types were similar.
- Under wave-current conditions the mean loads on the composite and aluminium blades were similar, in agreement with the results in current alone at the same average flow velocity.
- In wave-current flow when considering the time domain the amplitude of the average loading range per wave period was significantly reduced when operating the turbine with the composite blades compared to the rigid aluminium blades. The thrust and torque fluctuations were reduced by up to 10% and 14% respectively.

- These reductions in the average loading range per wave period increased with the rotational speed of the turbine, and hence the loads acting on the blades increased inducing a greater bend-twist response.
- The magnitude of the thrust fluctuations associated with the frequency of rotation of the turbine was greater for the composite blades compared to the rigid aluminium blades in all conditions tested (current and wave-current) due to their higher flexibility. However, the magnitude of these fluctuations was small compared to both the average value of thrust, and to the fluctuations associated with waves, and hence the fluctuations at the wave frequency dominated the overall blade response in wave-current flow.

This study has demonstrated the potential for bend-twist blades to passively damp fluctuations in power and thrust due to waves. Shedding of excess thrust loads will help to increase blade fatigue life and reduce the probability of failure of the blades and drivetrain components. It may also lead to a reduction in the cost of components through tailoring of the design load specifications. Damping of the power fluctuations will be of benefit to the design of the generator and power conditioning unit, increasing their cost effectiveness due to the reduction in peak loads and improved power smoothing.

Continuing research into the performance of bend-twist blades is needed to fully optimise them for the tidal energy application at full scale so that the desired power and thrust curves are realised in tandem with a suitable structural design. Following this the cost of manufacture of this type of blade compared to more conventional options needs to be determined so that the potential for capital and maintenance cost reductions can be properly assessed.

To move towards this goal, in the nearer term future work will investigate the bend-twist performance of composite blades in a wider range of wave and current conditions, including extreme events, so that bend-twist is induced for a greater portion of the wave cycle and faster flow velocities where the benefits of bend-twist blades can be further visualised. The axial loads on the rotor plane and on individual blades will also be compared with the rotor loads discussed in this study to better understand the blade structural performance and interaction effects between the wave period and turbine rotational period. Blade deflections will be measured during testing to directly monitor the bend-twist response, similar to the work presented in [18]. Moreover, blade deformations in non-uniform flow fields should be taken into account by performing a hydro-elastic deformation study. Alongside this, the numerical modelling work presented in [34] will be extended to include wave-current conditions and compared with the experimental results from this study, so as to develop a more comprehensive design tool for composite bend-twist tidal turbine blades.

ACKNOWLEDGEMENTS

This research was funded under the EPSRC Supergen UKCMER Grand Challenges project 'Reducing the costs of marine renewables via advanced structural materials' [grant EP/K013319/1]. Thank you to the team at IFREMER for their support during the testing period. The authors also thank Airborne Marine (Netherlands) for blade manufacturing, Natural Sciences and Engineering Research Council of Canada, Killam Trust, Offshore Energy Research Association of Nova Scotia, United Kingdom Science and Innovation, and Scottish Development International for funding.

REFERENCES

[1] G. Evans, "Maintaining marine turbines," 2013 . [Online]. Available: http://www.power-technology.com/features/feature-maintaining-marine-turbines-tidal-energy/. [Accessed 02 06 2017].

[2] I. A. Milne, R. N. Sharma, R. G. J. Flay and S. Bickerton, "Characteristics of the turbulence in the flow at a tidal stream power site.," *Phil Trans R Soc A 371: 20120196.,* 2013.

[3] T. Nevalainen, The effect of unsteady sea conditions on tidal stream turbine loads and durability. PhD Thesis., Glasgow, UK: The University of Strathclyde, 2016.

[4] J. King and T. Tryfonas, *Tidal stream power technology - state of the art,* IEEE, 2009.

[5] H. Kooijman, "Bending-torsion coupling of a wind turbine rotor blade, Report no. ECN-I--96-060," École Centrale de Nantes (ECN), Nantes, 1998.

[6] J. R. Xiao, B. A. Gama and J. W. Gillespie, "Progressive damage and delamination in plain weave S-2 glass/SC-15 composites under quasi-static punch-shear loading," *Composite Structures,* vol. 78, pp. 182-196, 4 2007.

[7] D. M. Grogan, S. B. Leen, C. R. Kennedy and C. M. Ó Brádaigh, "Design of composite tidal turbine blades," *Renewable Energy,* vol. 57, pp. 151-162, 9 2013.

[8] M. Mohan, "The advantages of composite material in marine renewable energy structures," in *RINA Marine Renewable Energy Conference*, 2008.

[9] R. Murray, Passively adaptive tidal turbine blades: design methodology and experimental testing, PhD thesis, Dalhousie : Dalhousie University, 2016.

[10] R. E. Murray, T. Nevalainen, K. Gracie-Orr, D. A. Doman, M. J. Pegg and C. M. Johnstone, "Passively adaptive tidal turbine blades: Design tool development and initial verification," *International Journal of Marine Energy,* vol. 14, pp. 101-124, 6 2016.

[11] R. F. Nicholls-Lee and S. R. Turnock, *Enhancing Performance of a Horizontal Axis Tidal Turbine using Adaptive Blades,* IEEE, 2007.

[12] M. R. Motley and R. B. Barber, "Passive control of marine hydrokinetic turbine blades," *Composite Structures,* vol. 110, pp. 133-139, 4 2014.

[13] R. B. Barber and M. R. Motley, "A numerical study of the effect of passive control on cavitation for marine hydrokinetic turbines," in *11th European Wave and Tidal Energy Conference*, Nantes, France, 2015.

[14] B. Gaurier, P. Davies, A. Deuff and G. Germain, "Flume tank characterization of marine current turbine blade behaviour under current and wave loading," *Renewable Energy,* vol. 59, pp. 1-12, 11 2013.

[15] N. Barltrop, K. S. Varyani, A. Grant, D. Clelland and X. P. Pham, "Investigation into wave--current interactions in marine current turbines," *Proceedings of the Institution of Mechanical Engineers, Part A: Journal of Power and Energy,* vol. 221, pp. 233-242, 3 2007.

[16] T. A. Jesus Henriques, S. C. Tedds, A. Botsari, G. Najafian, T. S. Hedges, C. J. Sutcliffe, I. Owen and R. J. Poole, "The effects of wave-current interaction on the performance of a model horizontal axis tidal turbine," *International Journal of Marine Energy,* vol. 8, pp. 17-35, 12 2014.

[17] P. Galloway, L. Myers and A. A. Bahaj, "Quantifying wave and yaw effects on a scale tidal stream turbine," *Renewable Energy,* vol. 63, pp. 297-307, 2014.

[18] S. Ordonez-Sanchez, M. Allmark, K. Porter, R. Ellis, C. Lloyd, I. Santic, T. O'Doherty and C. Johnstone, "Analysis of a Horizontal-Axis Tidal Turbine Performance in the Presence of Regular and Irregular Waves Using Two Control Strategies," *Energies,* vol. 12, no. 3, 2019.

[19] R. M. Mejia, G. S. Payne and T. Bruce, "The effects of oblique waves and currents on the loadings and performance of tidal turbines.," *Ocean Engineering,* vol. 164, pp. 55-64, 2018.

[20] S. Draycott, G. Payne, J. Steynor, A. Nambiar, B. Sellar and V. Venugopal, "An experimental investigation into non-linear wave loading on horizontal axis tidal turbines," *Journal of Fluids and Structures,* pp. 199-217, 2019.

[21] S. Tatum, M. Allmark, C. Frost, D. O'Doherty, A. Mason-Jones and T. O'Doherty, "CFD modelling of a tidal stream turbine subjected to profiled flow and surface gravity waves," *International Journal of Marine Energy,* vol. 15, pp. 156-174, 9 2016.

[22] T. M. Nevalainen, C. M. Johnstone and A. D. Grant, "A sensitivity analysis on tidal stream turbine loads caused by operational, geometric design and inflow parameters," *International Journal of Marine Energy,* vol. 16, pp. 51-64, 12 2016.

[23] Y. L. Young, M. R. Motley and R. W. Yeung, "Three-Dimensional Numerical Modeling of the Transient Fluid-Structural Interaction Response of Tidal Turbines," *Journal of Offshore Mechanics and Arctic Engineering,* vol. 132, p. 011101, 2010.

[24] P. Liu and B. Veitch, "Design and optimization for strength and integrity of tidal turbine rotor blades," *Energy,* vol. 46, pp. 393-404, 10 2012.

[25] IFREMER, "Le laboratoire comportement des structures en mer (in French),," IFREMER, 2015. [Online]. Available: http://wwz.ifremer.fr/manchemerdunord/Technologie-marine. [Accessed 02 06 17].

[26] M. Allmark, R. Grosvenor and P. Prickett, "An approach to the characterisation of the performance of a tidal stream turbine," *Renewable Energy,* vol. 111, pp. 849-860, 2017.

[27] N. Kolekar and A. Banerjee, "Performance characterization and placement of a marine hydrokinetic turbine in a tidal channel under boundary proximity and blockage effects," *Applied Energy,* vol. 148, pp. 121-133, 2015.

[28] Bosch Rexroth AG, "Rexroth IndraDyn T Synchronous-Torquemotors, Project Planning Manual, Document no. 120-1500-B315-03/EN," Bosch Rexroth AG, Lohr am Main, Germany, 2005.

[29] M. R. Hashemi, S. P. Neill, P. E. Robins, A. G. Davies and M. J. Lewis, "Effect of waves on the tidal energy resource at a planned tidal stream array," *Renewable Energy,* vol. 75, pp. 626-639, 3 2015.

[30] J. GROENEWEG and G. KLOPMAN, "Changes of the mean velocity profiles in the combined wave-current motion described in a GLM formulation," *Journal of Fluid Mechanics,* vol. 370, pp. 271-296, 9 1998.

[31] M. Umeyama, "Changes in Turbulent Flow Structure under Combined Wave-Current Motions," *Journal of Waterway, Port, Coastal, and Ocean Engineering,* vol. 135, pp. 213-227, 9 2009.

[32] P. H. Kemp and R. R. Simons, "The interaction between waves and a turbulent current: waves propagating with the current," *Journal of Fluid Mechanics,* vol. 116, pp. 227-250, 3 1982.

[33] T. Burton, N. Jenkins, D. Sharpe and E. Bossanyi, Wind energy handbook, Chichester: John Wiley & Sons Inc., 2001.

[34] R. E. Murray, S. Ordonez-Sanchez, K. E. Porter, D. A. Doman, M. J. Pegg and C. M. Johnstone, "Towing tank testing of passively adaptive composite tidal turbine blades and comparison to design tool," *Renewable Energy,* vol. 116, pp. 202-214, 2 2018.

[35] P. Mycek, B. Gaurier, G. Germain, G. Pinon and E. Rivoalen, "Experimental study of the turbulence intensity effects on marine current turbines behaviour. Part I: One single turbine," *Renewable Energy,* vol. 66, pp. 729-746, 6 2014.

[36] A. Mason-Jones, D. M. O'Doherty, C. E. Morris, T. O'Doherty, C. B. Byrne, P. W. Prickett, R. I. Grosvenor, I. Owen, S. Tedds and R. J. Poole, "Non-dimensional scaling of tidal stream turbines," *Energy,* vol. 44, pp. 820-829, 8 2012.

[37] J. McNaughton, S. Harper, R. Sinclair and B. Sellar, "Measuring and modelling the power curve of a commercial-scale tidal turbine,," in *11th European Wave and Tidal Energy Conference*, Nantes, France, 2015.

[38] S. Ordonez-Sanchez, K. Porter, C. Frost, M. Allmark, C. Johnstone and T. O'Doherty, "Effects of wave-current interactions on the performance of tidal stream turbines,," in *3rd Asian Wave and Tidal Energy Conference*, Singapore, 2016.

[39] Y. H. Zhang and A. Stacey, "Review and assessment of fatigue dara for offshore structural components containing through-thickness crack," in *MAE 2008 27th international Conference on Offshore Mechanics and Arctic Engineering*, Estoril, Portugal, 2008.

[40] T. Xu and R. Bea, "Load Shedding of Fatigue Fracture in Ship Structures," *Marine Structures,* vol. 10, pp. 49-80, 1997.

[41] T. McCombes, C. Johnstone, B. Holmes, L. Myers, A. Bahaj and J. Kofoed, "Best practice for tank testing of small marine energy devices, Deliverable D3.3," Equitable Testing and Evaluation of Marine Energy Extraction Devices in terms of Performance, Cost and Environmental Impact (EquiMar), 2010.

[42] ITTC, "Guide to the expression of uncertainty in experimental hydrodynamics," ITTC – Recommended Procedures and Guidelines, 25th International Towing Tank Conference, Fukuoka, Japan, 2008.

APPENDIX 1 UNCERTAINTY ANALYSIS

The error bars shown in Figure 7 and Figure 11 in Section 4 were computed following the guidelines for conducting an uncertainty analysis produced by EquiMar [41] and the ITTC [42]. The precision, bias, and combined expanded uncertainty values for the measured variables are given in Table 3. The bias uncertainties were obtained from manufacturer specifications, measurement equipment resolution, or calibration of the test equipment and are given in [34].

The precision uncertainty given in Table 3 equates to the standard deviation between the average values of each parameter from repeated test runs. The highest standard deviation in the thrust and torque occurred in the repeat set conducted with the aluminium blades at 75 RPM. Because of the low uncertainty in the current only (CO) flow condition with wave makers uninstalled (Table 3), the errors from this test set can be primarily attributed to those inherent in the thrust and torque measurement techniques. Therefore, these values have been taken as the precision uncertainty to be applied to all test cases. The combined expanded uncertainty in Table 3 is the square root of the sum of the precision and bias uncertainties squared, multiplied by a coverage factor of 2.2. The error bars in Figure 7 and Figure 11 in Section 4 represent this parameter.

Table 3: Precision, bias and combined expanded uncertainty values based on the 0.8 m/s CO repeated test set with the highest standard deviation (four repeated runs at 75 rpm, aluminium blades). The uncertainty in the current only (CO), current with inactive wave makers installed (CM) and wave-current (WC) flow velocities calculated across all test runs is also given.

Uncertainty values	***Mean value***	***Precision***	***Bias***	***Combined expanded***	***Percent of mean value (%)***
Power (W)	35.42	2.03	N/A	4.47	12.62
Thrust (N)	79.68	2.82	0.02	6.20	7.78

Rotational speed (RPM)	74.97	0.02	0.20	0.44	0.59
CO flow velocity (m/s)	0.80	0.0014	0.0013	0.0042	0.53
WC flow velocity (m/s)	0.79	0.0014	0.0013	0.0042	0.53
CM flow velocity (m/s)	0.75	0.0100	0.0013	0.0222	2.96

In Table 3 the error in the torque is slightly higher than that in the thrust due to the greater variability in the calibration data (Figure 2). This is probably a consequence of employing an indirect method to obtain the rotor torque via the motor TGC. It is recommended in future test programs to install a torque transducer on the drive shaft to reduce this uncertainty. The higher uncertainty in the CM flow velocity compared to in the CO and wave-current cases is a direct result of the flow disturbances set-up by the inactive wave-maker positioned in the flume.